Molecular Cancer Research

AACR

Critical Role of Endogenous Heme Oxygenase 1 as a Tuner of the Invasive Potential of Prostate Cancer Cells

Geraldine Gueron, Adriana De Siervi, Mercedes Ferrando, et al.

Updated version	Access the most recent version of this article at: doi:10.1158/1541-7786.MCR-08-0325
Supplementary Material	Access the most recent supplemental material at: http://mcr.aacrjournals.org/content/suppl/2009/11/18/1541-7786.MCR-08-0325.DC1.html

Cited Articles	This article cites by 47 articles, 21 of which you can access for free at: http://mcr.aacrjournals.org/content/7/11/1745.full.html#ref-list-1
Citing articles	This article has been cited by 6 HighWire-hosted articles. Access the articles at: http://mcr.aacrjournals.org/content/7/11/1745.full.html#related-urls

E-mail alerts	Sign up to receive free email-alerts related to this article or journal.
Reprints and Subscriptions	To order reprints of this article or to subscribe to the journal, contact the AACR Publications Department at pubs@aacr.org.
Permissions	To request permission to re-use all or part of this article, contact the AACR Publications Department at permissions@aacr.org.

Critical Role of Endogenous Heme Oxygenase 1 as a Tuner of the Invasive Potential of Prostate Cancer Cells

Geraldine Gueron,[1] Adriana De Siervi,[1] Mercedes Ferrando,[1] Marcelo Salierno,[2] Paola De Luca,[1] Belen Elguero,[1] Roberto Meiss,[3] Nora Navone,[4] and Elba S. Vazquez[1]

[1]Department of Biological Chemistry, School of Sciences, University of Buenos Aires, [2]Department of Inorganic, Analytical, and Physical Chemistry, Ciudad Universitaria, CONICET, [3]Department of Pathology, Institute of Oncological Studies, National Academy of Medicine, Buenos Aires, Argentina; and
[4]Department of Genitourinary Medical Oncology, The University of Texas,
M.D. Anderson Cancer Center, Houston, Texas

Abstract

Prostate cancer (PCa) is the second leading cause of cancer-associated death in men. Inflammation has been recognized as a risk factor for this disease. Heme oxygenase 1 (HO-1), the inducible isoform of the rate-limiting enzyme in heme degradation, counteracts oxidative and inflammatory damage. Here, we investigated the regulated expression of HO-1 and its functional consequences in PCa. We studied the effect of genetic and pharmacologic disruption of HO-1 in the growth, invasion, and migration in androgen-sensitive (MDA PCa2b and LNCaP) and androgen-insensitive (PC3) PCa cell lines. Our results show that HO-1 levels are markedly decreased in PC3 compared with MDA PCa2b and LNCaP. Hemin treatment increased HO-1 at both protein and mRNA levels in all cell lines and decreased cell proliferation and invasion. Furthermore, overexpression of HO-1 in PC3 resulted in markedly reduced cell proliferation and migration. Accordingly, small interfering RNA–mediated silencing of HO-1 expression in MDA PCa2b cells resulted in increased proliferation and invasion. Using reverse transcription-quantitative PCR–generated gene array, a set of inflammatory and angiogenic genes were upregulated or downregulated in response to HO-1 overexpression identifying matrix metalloprotease 9 (MMP9) as a novel downstream target of HO-1. MMP9 production and activity was downregulated by HO-1 overexpression. Furthermore, PC3 cells stably transfected with HO-1 (PC3HO-1) and controls were injected into nu/nu mice for analysis of in vivo tumor xenograft phenotype. Tumor growth and MMP9 expression was significantly reduced in PC3HO-1 tumors compared with control xenografts. Taken together, these results implicate HO-1 in PCa cell migration and proliferation suggesting its potential role as a therapeutic target in clinical settings. (Mol Cancer Res 2009;7(11):1745–55)

Introduction

Prostate cancer (PCa), one of the most common cancers in men, is considered a lethal malignancy with increasing incidence worldwide (1). The pathogenesis of PCa reflects both hereditary and environmental components. It has recently been recognized that inflammation, triggered by infectious agents or exposure to environmental factors, increases PCa tumorigenesis (2). The molecular mechanisms that underlie the pathogenesis of cancer-associated inflammation are complex and involved a delicate interplay between Th1, Th17, and CD8+ effector cells and several types of T-regulatory cells in the tumor microenvironment (3). Cytokines, chemokines, and matrix metalloproteases (MMP) constitute a proinflammatory network that directly contributes to malignant progression (4). Several chemokines were found to be elevated in prostate cancer, a phenomenon which might be coupled to tumor growth and local invasion (5). Enhanced MMP expression and activity has been correlated with PCa invasion, angiogenesis, and metastasis (6, 7). In addition, highly reactive chemical compounds, such as reactive oxygen species, produced during inflammation, could cause oxidative damage to DNA in epithelial cells or react with other cellular components initiating a free radical chain reaction (8), thus sustaining the prostate carcinogenic process (2).

Heme oxygenases are the rate-limiting enzymes in heme degradation that catalyze the conversion of heme into carbon monoxide, iron, and biliverdin. Heme oxygenase 1 (HO-1) has protective functions and its anti-inflammatory, antiapoptotic, and antiproliferative capacities have been observed in several cell types (9). Accumulating evidence indicates that HO-1 controls cell growth and proliferation in a cell-specific manner (10). Hemin, a potent inducer of HO-1, mitigates inflammation via upregulation of HO-1, which correlates with reduced levels of proinflammatory cytokines (11-13). HO-1 exerts its anti-inflammatory effects by inhibiting leukocyte transendothelial migration during complement-dependent inflammation (14). In a lipopolysaccharide-induced inflammatory angiogenesis, induction of HO-1 significantly inhibited leukocyte recruitment (15). Hence, induction of HO-1 represents a key event in cellular responses to pro-oxidative and proinflammatory insults (16).

FIGURE 1. HO-1 expression in prostate cancer cells and hemin induction. **A.** Western blot analysis showing differential basal expression of HO-1 in PC3, LNCaP, and MDA PCa2b. HO-1 induction by hemin was analyzed in PC3, LNCaP, and MDA PCa2b at the protein level. Cells were cultured for 48 h and then were exposed to hemin (30-80 μmol/L) for 24 h. Total protein was extracted, and HO-1 expression was analyzed by Western blotting. Recombinant HO-1 was used as positive control. β-Actin levels are shown to control for equal loading. **B.** Hemin-induced HO-1 mRNA in PCa cell lines. PC3, LNCaP, and MDA PCa2b cells were exposed to hemin (70 μmol/L, 24 h). Total RNA was extracted, and HO-1 mRNA levels were analyzed by real-time PCR. Data were normalized to β-actin. One representative from at least three independent experiments is shown (*, $P < 0.01$, significant difference). **C.** Minimal HO-1 promoter region regulated by hemin. PC3 and LNCaP cells were transfected with the 4.9 kb promoter region of *ho1* human wild-type or the same promoter region with the HO-CRE and MARE sequences mutated (HO4.9_M1LUC or HO4.9_M2LUC, respectively). After transfection, cells were maintained in complete medium (control) or stimulated with hemin (70μmol/L), lysed, and luciferase activity assay was done. Data were normalized to protein values. One representative from at least three independent experiments is shown (*, $P < 0.05$, significant difference).

HO-1 has been detected in several cancer cell lines (17-19) and tumors (20-24), but its functional relevance is still controversial. Recently, we have reported the expression of HO-1 in human PCa (25). These findings have shown, for the first time, that HO-1 expression and nuclear localization can define a new subgroup of prostate cancer primary tumors and that the modulation of HO-1 expression and its nuclear translocation could represent new avenues for therapy.

Here, we investigated the expression of HO-1 in androgen-sensitive and androgen-insensitive PCa cell lines and assessed whether its chemical or genetic disruption *in vitro* favored changes in cell proliferation, invasion, and migration. Furthermore, we also examined whether HO-1 expression might affect *in vivo* tumor growth by generating PC3 xenografts in *nu/nu* mice.

Results

HO-1 Expression in Androgen-Sensitive and -Insensitive Prostate Cancer Cell Lines

The endogenous expression levels of HO-1 protein were examined in three PCa cell lines: PC3 (derived from a bone metastasis, androgen-insensitive), LNCaP (derived from a lymph node metastasis, androgen-sensitive), and MDA PCa2b (derived from a bone metastasis, androgen-sensitive). We found high HO-1 expression in androgen-sensitive cell lines with the highest levels observed in MDA PCa2b (Fig. 1A). The androgen response triggers oxidative stress (26), and therefore, the high endogenous expression of HO-1 in LNCaP and MDA PCa2b cell lines may be associated with the maintenance of a homeostatic response.

Hemin Induces HO-1 Expression in Prostate Cancer Cell Lines

To investigate the functional relevance and regulated expression of HO-1, we further explored the ability of hemin to induce HO-1 expression in PCa cell lines. Treatment of MDA PCa2b, LNCaP, and PC3 cells with hemin resulted in greatly enhanced HO-1 expression at the protein level (Fig. 1B). Remarkably, reverse transcription-quantitative PCR (RT-qPCR) revealed a 36.8-fold induction of HO-1 mRNA in PC3 cell line, whereas a 3.9-fold and a 6.3-fold induction was observed in LNCaP and MDA PCa2b, respectively (Fig. 1B). MTS assay showed that cell viability was not affected by hemin at any concentration tested in all cell lines (data not shown). These results show that HO-1 may be chemically modulated in both hormone-sensitive and hormone-insensitive PCa cell lines. Moreover, the transcriptional activity of the HO-1 promoter (4.9 kb upstream of the HO-1 transcription start site: hHO4.9luc) was significantly induced by hemin in PC3 and LNCaP (Fig. 1C). A construct containing the CRE site–mutated (hHO4.9_M1luc) or the MARE site–mutated (hHO4.9_M2luc), both antioxidant
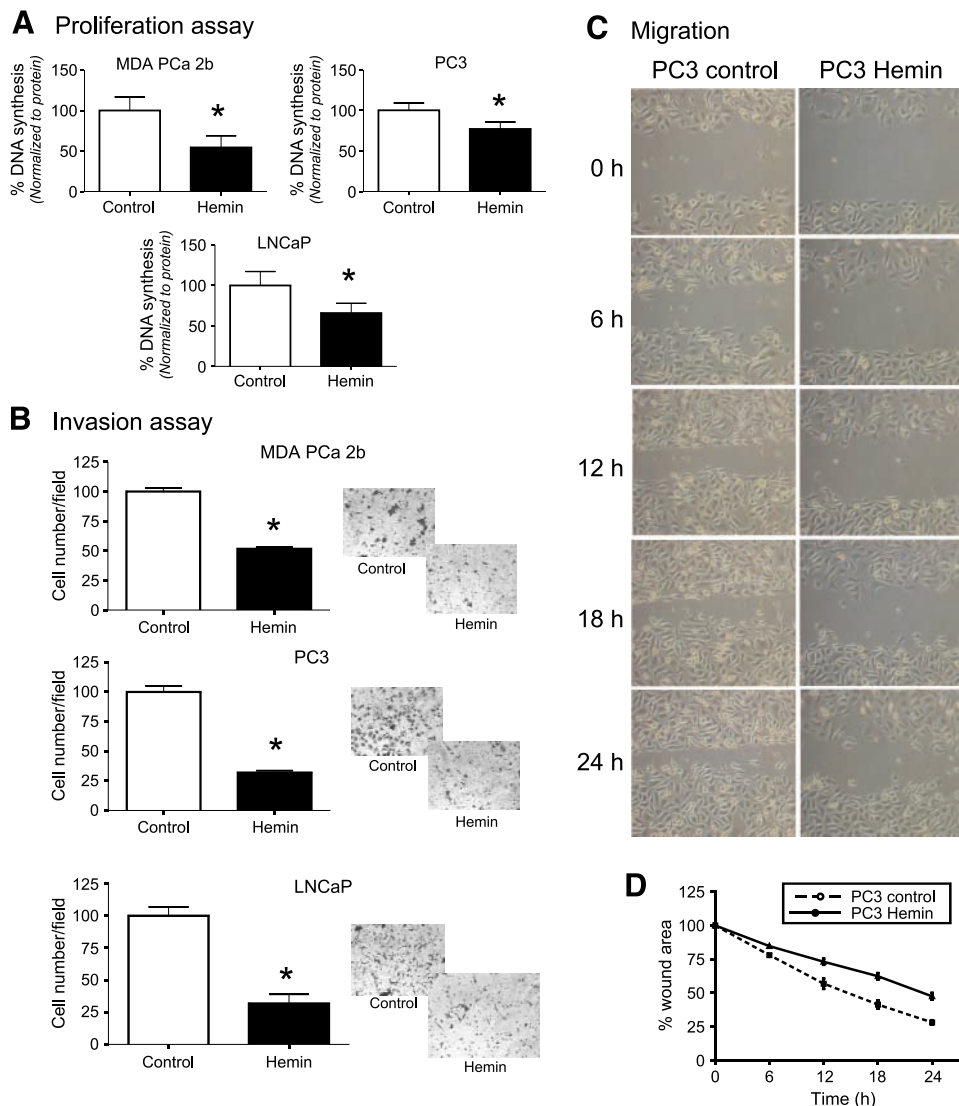

FIGURE 2. Hemin inhibits prostate cancer cell proliferation, invasion, and migration. **A.** PC3, LNCaP, and MDA PCa2b cell proliferation was measured by [³H]thymidine incorporation after 24 h of incubation with or without hemin (70 μmol/L). One representative from at least three independent experiments is shown (*columns,* mean of triplicates; *bars,* SD; *, $P < 0.05$, significant difference). **B.** PC3, LNCaP, and MDA PCa2b cell invasion was measured using Matrigel-coated transwell culture inserts. Cells were seeded into the upper chambers and hemin (70 μmol/L) was included or not, as indicated. The bottom wells were filled with complete medium. Cells that had invaded to the underside of the inserts after 24 h of incubation were counted by light microscopy. Four fields of view from each insert were counted. One representative from at least three independent experiments is shown (*columns,* mean of eight fields of view; *bars,* SEM; *, $P < 0.05$, significant difference). **C.** Representative phase-contrast images of the wound-healing assay. PC3 cells were grown to confluence into a monolayer in 35 mm Petri dishes. A linear scratch wound was done along the culture plate and cells were time-lapse–monitored every minute for 24 h. **D.** The uncovered wound area was measured at different intervals for 24 h and quantified using ImageJ 1.37v software (NIH). The graph represents the percentage of uncovered wound area taking the value at 0 h as 100%. The migration rate was calculated as the slope of free wound area/time (*points,* mean of two independent experiments; *bars,* SD).

response elements, completely abrogated hemin induction of luciferase activity in both cell lines (Fig. 1C), suggesting that both antioxidant response elements are required for HO-1 induction by hemin. Altogether, these results indicate that HO-1 is regulated by hemin at the transcriptional and protein levels in PCa cells.

Hemin Decreases Proliferation and Invasion in Prostate Cancer Cells

To investigate whether HO-1 upregulation has an effect on PCa cell proliferation, we assessed ^{3}H-thymidine incorporation in hemin-treated and untreated cells. A significant decrease in cell proliferation was observed in hemin-treated PC3 (23%, $P < 0.05$), LNCaP (34.07%, $P < 0.05$), and MDA PCa2b cells (45.5%, $P < 0.05$; Fig. 2A). Moreover, hemin treatment significantly reduced the invasiveness of PC3 (68%, $P < 0.05$), LNCAP (68.13% $P < 0.05\%$), and MDA PCa2b cells (51.7%, $P < 0.05$) when compared with their untreated controls (Fig. 2B).

Hemin Decreases Migration in Androgen-Insensitive Prostate Cancer Cells

To evaluate the migratory capacity of PCa cells, we used an *in vitro* scratch wound assay. Confluent monolayers of hemin-treated or untreated PC3 and MDA PCa2b cells were wounded. Wound closure was time-lapse–monitored every minute for 24 h as previously described (27). Untreated PC3 cells migrated and almost covered the wound by 24 hours (uncovered wound area, 28.18%), whereas in hemin-treated PC3 cells, a significant area of the wound (47.6%) remained uncovered over the same period (Fig. 2C; Supplementary Videos 1 and 2). This finding is also illustrated as the migration rate (calculated as the slope of free wound area / time; Fig. 2D) of PC3 control (slope = 3) and hemin-treated PC3 cells (slope = 2.1). In contrast, MDA PCa2b cells expressing high levels of endogenous HO-1 were unable to migrate during the time of the assay (Supplementary Video 3) and no changes in their migratory capacity were observed upon hemin treatment (data not shown). These results suggest that high basal HO-1 levels may reduce the migratory capacity of PCa cell lines.
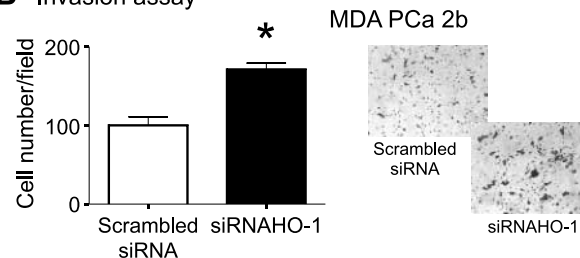
Endogenous HO-1 Inhibits Proliferation, Migration, and the Invasive Capacity of Prostate Cancer Cells

To examine whether inhibition of proliferation, migration, and invasiveness is in fact due to HO-1 overexpression, we first generated stably transfected PC3 cells with pcDNA3HO-1 (PC3HO-1) or with pcDNA3 as control (PC3pcDNA3) and checked for HO-1 expression by Western blot and RT-qPCR (Supplementary Fig. S3). HO-1 overexpression in PC3 decreased cell proliferation (42%; Fig. 3A), reduced cell migration (uncovered wound area after 24 hours, 75.82% versus 28.2%, PC3pcDNA3 and PC3HO-1, respectively) and the migration rate (PC3pcDNA3 slope = 3 versus PC3HO-1 slope = 0.98; Fig. 3C). However, no changes were observed in the invasive potential of these cells (data not shown). Because MDA PCa2b cells already express substantial levels of HO-1, we sought to knock down HO-1 *in vitro* using HO-1 small interfering RNA (siRNA). Noteworthy, siRNA-mediated silencing of HO-1 mRNA levels (>70%; Supplementary Fig. S3) significantly enhanced cell proliferation and upregulated the invasive
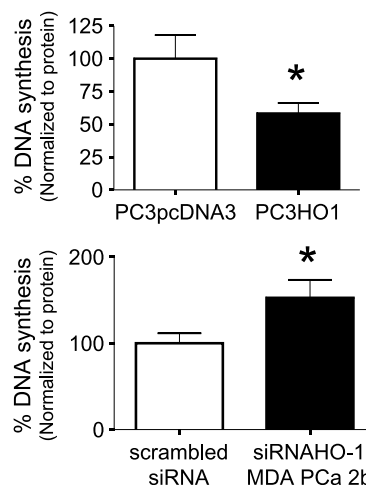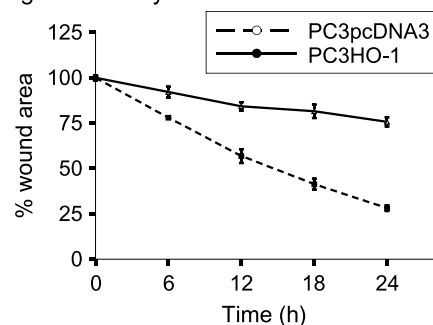

FIGURE 3. HO-1 inhibits proliferation, migration, and invasion in prostate cancer cells. **A.** PC3 cells were stably transfected with pcDNA3HO-1 (PC3HO-1) or pcDNA3 (PC3pcDNA3) expression vectors. MDA PCa2b cells were transfected with siRNAHO-1 or scrambled siRNA. PC3pcDNA3, PC3HO-1, MDA PCa2b scrambled siRNA, and MDA PCa2b siRNAHO-1 cells were grown for 48 h and cell proliferation was measured by [^{3}H]thymidine incorporation. One representative from at least three independent experiments is shown (*columns,* mean of triplicates; *bars,* SD; *, $P < 0.05$, significant difference). **B.** MDA PCa2b scrambled siRNA and MDA PCa2b siRNAHO-1 cells were grown for 48 h and cell invasion was measured using Matrigel-coated transwell inserts. Cells that had invaded to the underside of the inserts after 24 h of incubation were counted by light microscopy. Four fields of view from each insert were counted. One representative from at least three independent experiments is shown (*columns,* mean of eight fields of view; *bars,* SEM; *, $P < 0.05$, significant difference). **C.** PC3pcDNA3 and PC3HO-1 cells were grown to confluence into a monolayer in 35 mm Petri dishes. A linear scratch wound was done along the culture plate and cells were time-lapse–monitored every minute for 24 h. The uncovered wound area was measured at different intervals for 24 h and quantified using ImageJ 1.37v software (NIH). The graph represents the percentage of uncovered wound area taking the value at 0 h as 100%. The migration rate was calculated as the slope of free wound area/time (*points,* the mean of two independent experiments; *bars,* SD).

potential (50% and 71%, respectively; $P < 0.05$) of MDA PCa2b cells (Fig. 3A and B). However, no detectable changes were observed in the migration of MDA PCa2b cells under similar conditions (Supplementary Video 4). Given the apparent strong antimigratory effect of HO-1 and the high basal levels in MDA PCa2b cells, a further reduction on HO-1 may be required to achieve an effect in the migration properties of these cells. In addition, the technique may not be sensitive enough for the detection of very small changes in cell kinetics.

Identification of Potential HO-1 Gene Targets

To identify potential HO-1 gene targets which may provide an alternative mechanism for the observed effects, we analyzed the differential gene expression profile of MDA PCa2b and PC3 cells, focusing mainly on genes implicated in inflammation and angiogenesis. A total of 55 of the 113 genes were assessed which showed a difference of at least 2-fold between the expression values of the androgen-sensitive and the androgen-insensitive cell line (Fig. 4; Supplementary Table S1). Matching downregulated genes were observed between MDA PCa2b compared with PC3 and PC3HO-1 compared with PC3pcDNA3 including angiopoietin 1 (*ANGPT1*), angiopoietin-like 3 (*ANGPTL3*), the chemokines (*CXCL1, CXCL10, CXCL3,* and *CXCL5*), c-*fos*–induced growth factor (*FIGF*), interleukin 6 (*IL-6*), interleukin 8 (*IL-8*), MMP9, thrombospondin 1 (*THBS1*), and vascular endothelial growth factor A (*VEGFA*). On the other hand, only inhibitor of DNA binding 3 protein (ID3) was upregulated when comparing MDA PCa2b to PC3 and PC3HO-1 to PC3pcDNA3. Similar findings were obtained in a second independent experiment. These results suggest that genes involved in inflammation and angiogenesis are mainly associated with overexpression of HO-1.

HO-1 Decreases MMP9 Expression and Activity in Androgen-Insensitive Prostate Cancer Cells

We subsequently focused our studies on MMP9 because this metalloproteinase has been implicated together with other MMPs in cancer cell migration and invasion (28). The gene array showed that the expression of MMP9 was lower in MDA PCa2b (35-fold) compared with PC3 and PC3HO-1 (9.7-fold) compared with PC3pcDNA3 (Fig. 4; Supplementary Table S1) suggesting a negative correlation between MMP9 and HO-1 expression. Downregulation of MMP9 expression in PC3HO-1 was further confirmed by RT-qPCR (Fig. 5A). Moreover, hemin treatment in MDA PCa2b and LNCaP cell lines significantly reduced MMP9 expression at the transcriptional level (85.55% in LNCaP, $P < 0.05$; 26.29% in MDA PCa2b, $P < 0.05$) when compared with their untreated controls (Fig. 5B). The percentage of decrease in MMP9 expression in MDA PCa2b was lower than in LNCaP as expected, given the high HO-1 endogenous levels of this cell line.

To determine the effects of HO-1 overexpression on MMP9 activity, we collected conditioned medium from PC3HO-1 and PC3pcDNA3 cells and a zymographic analysis was done. A significant decrease (44.1%, $P < 0.05$) in MMP9 activity in HO-1–transfected cells (Fig. 5C) was observed. These results clearly indicate that overexpression of HO-1 correlates with decreased MMP9 expression and activity in PC3 cells.
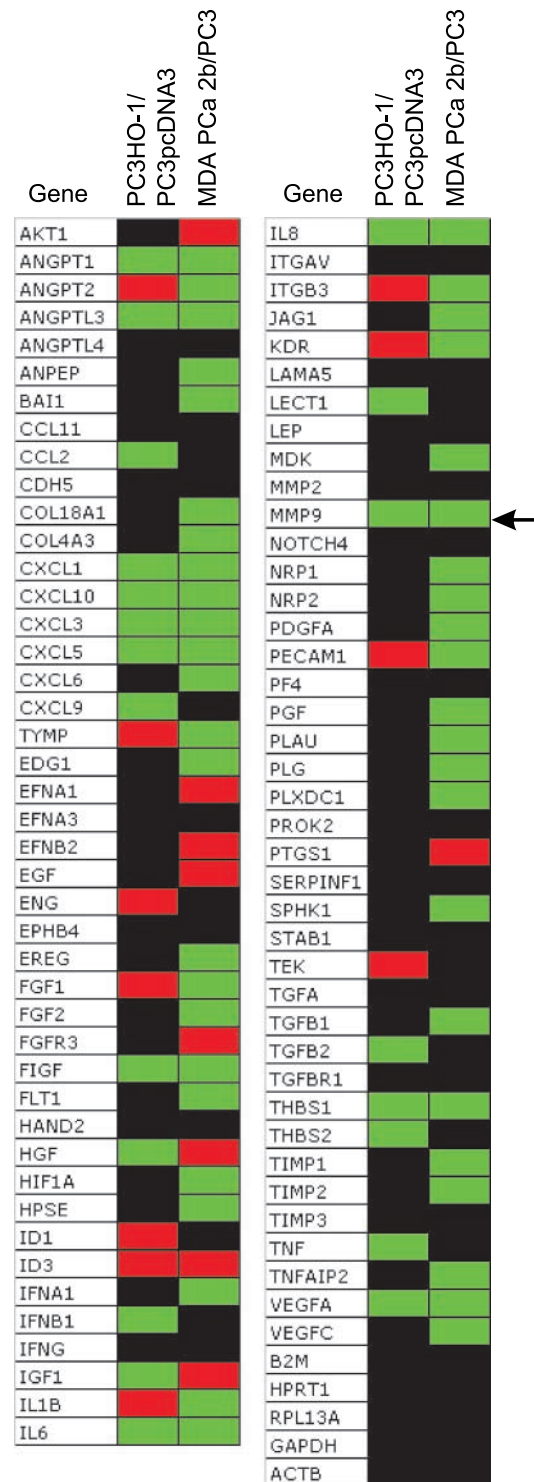
FIGURE 4. Identification of genes and gene sets likely to be regulated by HO-1 by microarray analysis. RT-qPCR Oligo GEArray Human Angiogenesis Microarray analysis was done for RNA samples from PC3, MDA PCa2b, PC3pcDNA3, and PC3HO-1. Data were normalized to B2M, HPRT1, RPL13A, GAPDH, and ACTB genes and two independent experiments were done. Comparisons between MDA PCa2b versus PC3 and PC3HO-1 versus PC3pcDNA3 were analyzed. Genes with expression levels higher than 2 were considered upregulated (*red boxes*), lower than −2 were considered repressed (*green boxes*), or genes with no significant difference between comparisons (*black boxes*).

FIGURE 5. HO-1 overexpression modulates MMP9 expression and activity in prostate cancer cells. **A.** PC3pcDNA3, PC3HO-1, and MDA PCa2b scrambled siRNA and MDA PCa2b siRNAHO-1 cells were cultured in complete medium for 48 h, and then total RNA was extracted. MMP9 mRNA levels were analyzed by real-time PCR. Data were normalized to β-actin. One representati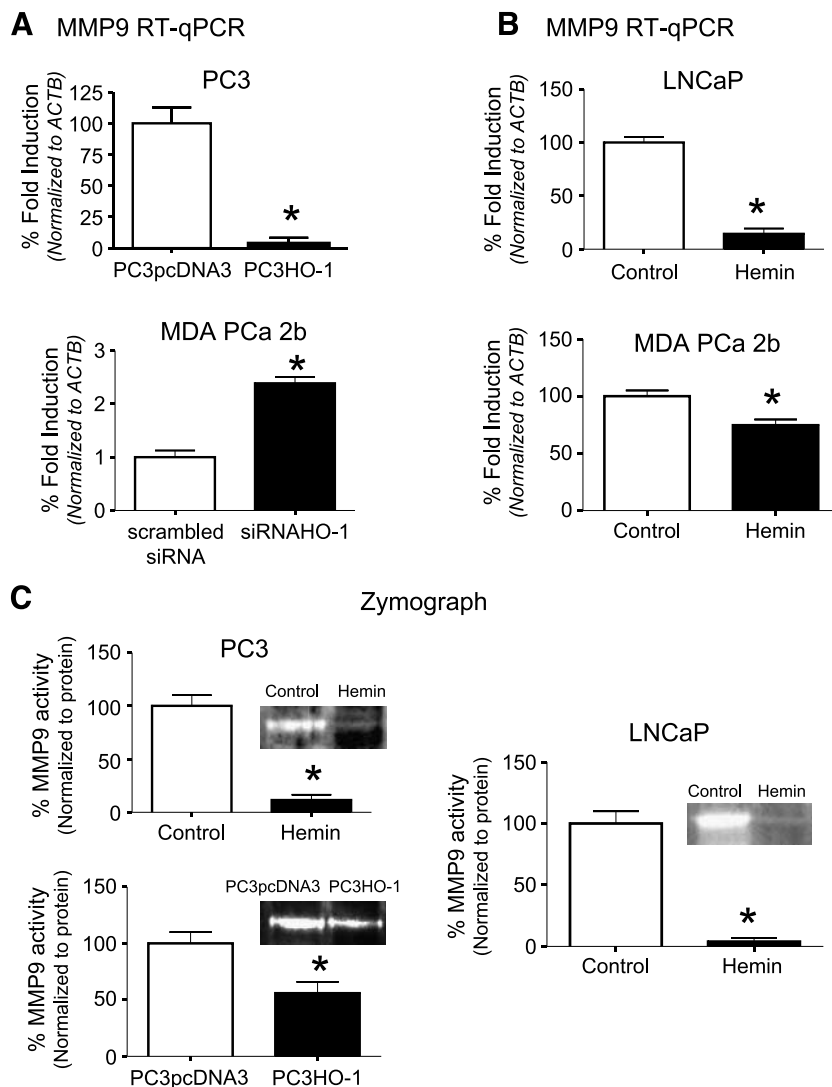ve from at least three independent experiments is shown (*, $P < 0.01$, significant difference). **B.** LNCaP and MDA PCa2b cells were treated with hemin (70 μmol/L) for 24 h, and then total RNA was extracted. MMP9 mRNA levels were analyzed by real-time PCR. Data were normalized to β-actin. One representative from at least three independent experiments is shown (*, $P < 0.01$, significant difference). **C.** Gelatin zymography was done on conditioned media from PC3pcDNA3, PC3HO-1, PC3, PC3 treated with hemin, LNCaP and LNCaP treated with hemin to assess MMP9 activity. Clear bands were quantified using ImageJ 1.37.v software (NIH) and normalized to total protein. One representative from three independent experiments is shown (*, $P < 0.05$, significant difference).

To further document the role of HO-1 in MMP9 expression, we depleted HO-1 in MDA PCa2b by siRNA-mediated strategies. The decrease of HO-1 resulted in a more than 2-fold increase in MMP9 mRNA, as detected by RT-qPCR analysis (Fig. 5A). Therefore, inhibition of HO-1 expression resulted in the upregulation of MMP9 expression. Finally, we assessed the effect of hemin on MMP9 activity and a striking 88.5% and 96.11% reduction in PC3 and LNCaP, respectively, was observed by zymography (Fig. 5C). These results further confirm that MMP9 is significantly modulated by HO-1. Thus, MMP9 is a downstream target of HO-1 in PCa cells.

Downregulation of MMP9 Expression Correlates with Reduced Growth of HO-1 Overexpressing Prostate Cancer Xenografts

To further determine the role of HO-1 *in vivo*, we injected s.c. 3.5×10^6 PC3HO-1 and PC3pcDNA3 cells in the right flank of athymic nude *nu/nu* male mice. Tumors developed in all mice injected. Their volumes were measured every 2 days starting at 8 days after inoculation, when the tumors became detect-

able under the skin. No significant difference was observed in body weight for mice bearing PC3HO-1 and PC3pcDNA3 tumors (data not shown). Tumor growth was reduced by an average of 58.6% ($P < 0.05$) in PC3HO-1–bearing mice (volume, 49 mm^3) 23 days after xenograft generation, compared with tumors induced by PC3pcDNA3 (volume, 118 mm^3; Fig. 6A). Furthermore, in tumors of both groups, mitotic figures of normal and abnormal features were evident; showing a reduced mitotic index in PC3HO-1 compared with PC3pcDNA3 [the mitosis per high–power field (40×) average was of 1 to 3 in PC3HO-1 tumors and of 4 to 6 in PC3pcDNA3 tumors; Fig. 6B], in accordance with the reduced proliferation rate observed in the *in vitro* assays (Fig. 2).

To investigate the levels of MMP9, mRNA was extracted from the tumors and RT-qPCR was done. MMP9 levels were significantly lower ($P < 0.05$) in PC3HO-1 xenografts compared with PC3pcDNA3 tumors (Fig. 6C). Furthermore, immunohistochemical analysis of PC3pcDNA3-generated tumors showed high MMP9 expression and negative HO-1 immunostaining. MMP9 immunoreactivity was exclusively cytoplasmic

and positive in five out of five tumors of PC3pcDNA3 group (Fig. 6D, *top left* and *middle*) whereas HO-1 expression was negative in five out of five tumors of the same group (Fig. 6D, *bottom left*). Conversely, no MMP9-positive immunostaining (zero out of five tumors) was detected in PC3HO-1 tumors (Fig. 6D, *top right*). Accordingly, HO-1 expression was positive in all the xenografts generated (five out of five) in the PC3HO-1 group (Fig. 6D, *middle* and *bottom right*). Cytoplasmatic and nuclear positive HO-1 was detected in PC3HO-1 tumors (Fig. 6D, *middle* and *bottom right*). The nuclear staining of HO-1 was further detected by Western blotting (data not shown), and confirmed our previous findings both in human primary prostate carcinomas and hemin-treated PCa cells (25). The results presented here clearly indicate that HO-1 plays an important role as an intermediate molecule connecting MMP9 and PCa progression.

Discussion

Understanding the biological mechanisms involved in androgen-independent tumor progression and metastasis has emerged as a fundamental issue in PCa research (2). Induction of HO-1 seems to be a fundamental cell defense process to insults from the environment such as stress stimuli (9). The anti-inflammatory effects of HO-1 seem to protect cells, tissues, and even whole organs from these environmental alterations. Murine cells lacking HO-1 are susceptible to the accumulation of free radicals and to oxidative injury *in vitro* and *in vivo* (29). Human HO-1 deficiency results in high levels of endothelial damage and prolonged inflammation (30, 31).

Different human cancers express high levels of HO-1 and controversial opinions have emerged on whether it provides growth advantages to tumor cells (32). Previous reports have associated HO-1 with prostate carcinogenesis (25, 33). However, the role of HO-1 in PCa has yet to be elucidated.

The data presented here shows that androgen-sensitive cell lines, MDA PCa2b and LNCaP, have higher endogenous levels of HO-1 compared with PC3 cells (Fig. 1A). Increasing evidence has shown that HO-1 participates in maintaining the cellular homeostasis (34). Therefore, the lack of HO-1 expression in PC3 could account for the augmented metastatic capacity reflected in its increased ability to proliferate, migrate, and invade. Thus, it is reasonable to hypothesize that HO-1 is implicated in the modulation of these cellular processes. We have shown that
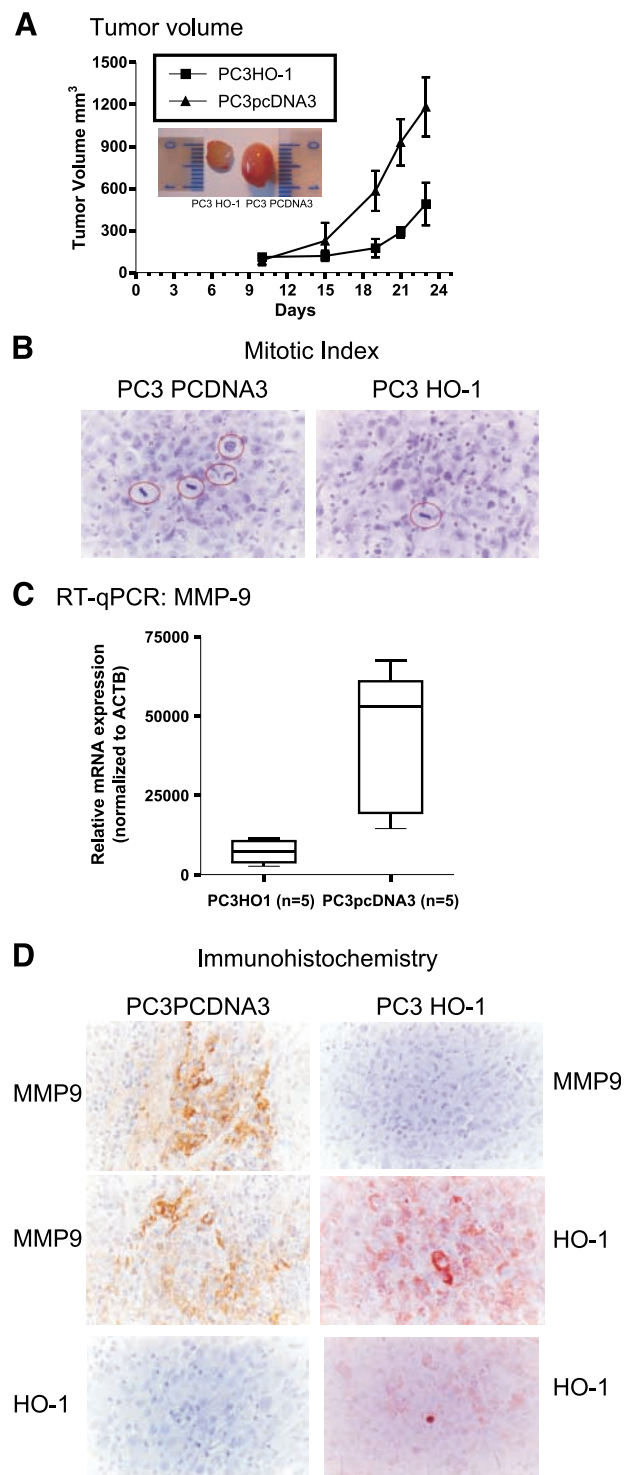

FIGURE 6. Downregulation of MMP9 expression correlates with reduced growth of HO-1 overexpressing PCa xenografts. **A.** Six- to 8-wk-old male athymic nude (*nu/nu*) mice were randomized into two groups: PC3HO-1 (*n* = 5) and PC3pcDNA3 (*n* = 5). Tumor cells (3.6 × 10^6) were injected s.c. in the right flank. Body weight and tumor growth were measured every 2 d starting at 8 d after inoculation when the tumors became detectable under the skin. Tumor volumes were calculated as described in Materials and Methods. **B.** Mitotic index, normal mitotic figures in PC3HO-1 tumor (H&E, 40×), average of one to three mitoses in PC3HO-1 tumors (*right*). Normal and abnormal mitotic figures in PC3pcDNA3 tumors (H&E, 40×), average of four to six mitoses in PC3pcDNA3 tumors (*left*). **C.** Harvested tumors (PC3HO-1 and PC3pcDNA3) were snap-frozen in liquid nitrogen and subsequently processed for RNA isolation. Total RNA was extracted, and MMP9 mRNA levels were analyzed by RT-qPCR. Data were normalized to β-actin. One representative from at least three independent experiments is shown (*, *P* < 0.05, significant difference). **D.** Immunohistochemical staining of HO-1 and MMP9 in PC3HO-1 and PC3pcDNA3 tumors. MMP9 intense cytoplasmic immunostaining in atypical cells in PC3pcDNA3 tumor and intense cytoplasmic immunostaining in a neoplastic nest outlying atypical cells (*top* and *middle left*). Negative immunostain for MMP9 in PC3HO-1 tumor (*top right*). Final magnification, ×500. HO-1 diffuse moderate to intense cytoplasmatic immunostain (*middle right*) and intense HO-1 nuclear immunostain in isolated cell from a PC3HO-1 tumor (*bottom right*). Negative immunostaining for HO-1 in PC3pcDNA3 tumor (*bottom left*). Final magnification, ×500.

hemin-induced HO-1 decreased the proliferation and invasion of PCa cells (Fig. 2). Moreover, we time-lapse–monitored PC3 cells and showed for the first time the reduced motility of these cells following hemin treatment (Fig. 2; Supplementary Videos 1 and 2). This observation is in accordance with the low motility observed in MDA PCa2b, which is likely to be related to the high basal expression of HO-1.

To elucidate the involvement of HO-1 in these cellular processes, we generated PC3HO-1 stably transfected clones and confirmed that HO-1 overexpression significantly reduced PC3 cell proliferation and migration (Fig. 3). However, no reduction in cell invasion could be detected. In addition to HO-1 induction, hemin modulates other genes as well (e.g., adhesion molecules), many of which influence important cellular processes (35). These could account for the differential invasive response of hemin-treated PC3 and PC3HO-1.

To assess the consequences of HO-1 deficiency, most studies have used synthetic heme analogues such as protoporphyrins, which are not specific for HO-1 and have the paradoxical effect of inducing HO-1 expression (32). Thus, we specifically knocked down HO-1 expression *in vitro* by siRNA-mediated strategies (36), which resulted in a significant increase of MDA PCa2b cell proliferation and invasion (Fig. 3). No modification in the reduced motility of these cells was detected by HO-1 silencing, probably due to the limitation of the technique to detect minor kinetic changes. Alternatively, the reduced levels of HO-1 induced by siRNA-mediated targeting were not sufficiently low to achieve an apparent increase in tumor cell motility. It is possible that HO-1 acts as a rheostat controlling cell proliferation, migration, and invasiveness in response to stress. Further kinetic studies will be necessary to address this issue.

The metastatic spread of PCa cells and the ability to survive when reaching the metastatic microenvironments is affected by growth factors, chemokines, adhesion molecules, angiogenic factors, and hormones (2). In this context, the present study sought to correlate the constitutive expression of genes associated with angiogenesis and inflammation in the MDA PCa2b and PC-3 cell lines, and analyze their expression following HO-1 genetic modulation. We identified a set of matching genes which were downregulated when comparing PC3HO-1 to PC3pcDNA3 and MDA PCa2b to PC3: *ANGPT1, ANGPTL3, CXCL1, CXCL3, CXCL10,* and *CXCL5, FIGF, IL6, IL8, MMP9, THBS1,* and *VEGFA*. On the other hand, only *ID3* was upregulated (Fig. 4). These data suggest that modulation of a set of genes implicated in angiogenesis and inflammation are directly related to HO-1 expression. Taking into account that the expression of HO-1 is regulated predominantly at the transcriptional level (32) and that recent studies have revealed the nuclear localization of the HO-1 protein pointing to its role as a potential transcription factor or coregulator (25, 37), further studies are warranted to investigate the potential signaling pathways triggered by HO-1 overexpression.

The MMPs are regulators of cell growth, migration, and extracellular matrix remodeling (38), and have been shown to be required for prostate tumor cell invasion and angiogenesis (6). Previous studies have linked MMPs to the metastatic potential of these cell lines and proposed the importance of finding specific target genes controlling MMPs (39). In the present report,

we identified MMP9 as a novel downstream target of HO-1 by demonstrating that HO-1 overexpression in PC3 and LNCaP cells markedly inhibited MMP9 expression and activity (Fig. 5). Moreover, HO-1 ablation in MDA PCa2b resulted in the upregulation of MMP9 expression (Fig. 5). These results further confirm that MMP9 is significantly modulated by HO-1. Recently, Notch1 was involved in human prostate cancer invasion and it was shown that silencing of NOTCH1 inhibited the invasion of human PCa cells by inhibiting the expression of MMP9 and urokinase plasminogen activator (40).

A striking finding of our study comes from the *in vivo* experiments. We found that tumor growth receded in PC3HO-1–bearing mice compared with tumors induced by PC3pcDNA3 (Fig. 6A). Furthermore, a reduced mitotic index was observed in PC3HO-1 compared with PC3pcDNA3 tumors (Fig. 6B), in accordance with the reduced proliferation rate observed *in vitro* (Fig. 3A). MMP9 levels were significantly lower ($P < 0.05$) in PC3HO-1 xenografts compared with PC3pcDNA3 tumors observed by RT-qPCR and immunohistochemistry analyses (Fig. 6C and D). Thus, downregulation of MMP9 expression correlates with the reduced growth of HO-1 overexpressing prostate tumor xenografts.

Very recently during the preparation of this article, Lin et al. (41) reported that HO-1 inhibited 12-*O*-tetradecanoylphorbol-13-acetate–induced invasion through suppressing MMP9 activity in breast cancer cells. Our observations are consistent with these findings and further extend to the identification of endogenous HO-1 expression in prostate cancer cells. Our finding reporting the downregulation of MMP9 by HO-1 in prostate cancer cells is of particular interest, and suggests, for the first time, that increased expression of HO-1 by prostate cancer cells could define a less invasive and therefore less aggressive phenotype. In this context, HO-1 could emerge as a novel prognostic target with potential clinical implications.

The overwhelming majority of PCa deaths occur in patients with metastases (6). Therapy of metastases should be focused not only on the intrinsic growth and survival properties of tumor cells, but also on the homeostatic factors that control tumor cell migration, invasiveness and angiogenesis. In this scenario, HO-1 emerges as a novel target for the prevention of PCa progression.

Materials and Methods

Cell Culture and Antibodies

LNCaP and PC3 cells were obtained from the American Type Culture Collection and were routinely cultured in RPMI 1640 (Invitrogen) supplemented with 10% fetal bovine serum. MDA PCa2b cells were propagated in BRFF-HPC1 medium (AthenaES), supplemented with 50 µg/mL of gentamicin, and 20% (v/v) fetal bovine serum. PC3HO-1 and PC3pcDNA3 were generated as described in Supplementary Methods. The antibody anti–HO-1 was from Stressgen Biotechnologies, Corp., anti–actin-β was from Sigma, and anti-mouse secondary antibody was from Amersham, Ltd.

Plasmids

hHO4.9luc, hHO4.9_M1luc, and hHO4.9_M2luc were kindly provided by Dr. N. Leitinger (Department of Vascular Biology and Thrombosis Research, University of Vienna,

Vienna, Austria). The human pcDNA3HO-1–expressing vector was kindly provided by Dr. M. Mayhofer (Clinical Institute for Medical and Chemical Laboratory Diagnostics, University of Vienna, Vienna, Austria).

siRNA Transfection

siRNA was synthesized in 2′-deprotected, duplexed, desalted, and purified form by Sigma. The sense and antisense sequences of human HO-1 siRNA were obtained from prior publications (refs. 42, 43; sense, 5′-GGAGAUUGAGCGCAA-CAAGdTdT-3′ and antisense 5′-CUUGUUGCGCUAAAU-CUCCdTdT-3′). siRNA scramble (Dharmacon) was used as a negative control. MDA PCa2b were grown in 60 mm plates until 50% to 60% of confluence and transfected using LipofectAMINE 2000 reagent (Invitrogen) in medium without fetal bovine serum. After 5 h of incubation, 20% fetal bovine serum/BRFF-HPC1 medium was added. Proliferation, invasion, and migration assays were done 72 h posttransfection.

Luciferase Assay

PC3 and LNCaP cells were transfected by the calcium phosphate method with the 4.9-kb promoter region of HO-1 human wild-type or the same promoter region with the HO-CRE and MARE sequences mutated (HO4.9_M1LUC or HO4.9_M2-LUC, respectively). After transfection, cells were maintained in complete medium (control) or stimulated with 70 μmol/L of hemin. Cells were then incubated in Reporter Lysis Buffer (Promega) and luciferase activity was determined by the Luciferase Assay system (Promega) in a HIDEX luminometer. Data were normalized to total protein determined by the Bradford assay.

Immunoblotting

PCa cells were treated or not with hemin (30-70 μmol/L, 24 h) and lysed with CelLytic M Cell Lysis Reagent (Sigma) and Western blot was done as described in Supplementary Methods.

Zymography

MMP9 activity was analyzed by gelatin zymography as described previously (44) and slightly modified (Supplementary Methods).

RNA Isolation and RT-qPCR

Total RNA was isolated with the RNeasy Mini Kit (Qiagen). cDNAs were synthesized with Omniscript Reverse Transcriptase (Qiagen) and used for real-time PCR amplification with Taq HotStart master mix kit (Qiagen; ref. 45). Primers were designed to amplify a 100-bp region present in the fully mature RNA species of HO-1 (5′-GAGTGTAAGGACCCATCGGA-3′ and 5′-GCCAGCAACAAAGTGCAAG-3′); MMP9 (5′-AGACCTGGGCAGATTCCAAACC-3′ and 5′-GCAAAGG-CGTCGTCAATCACC-3′); VEGFA (5′-GCCTTGCCTTGCT-GCTCTACC-3′ and 5′-GTGATGATTCTGCCCTCCTCC-TTC-3′); VEGFC (5′-AGGCTGGCAACATAACAGAGAAC-3′ and 5′-GCGACTCCAAACTCCTTCCC-3′) and ACTB (5′CGGTTGGCCTTAGGGTTCAGGGGGG-3′ and 5′-GTGGG-CCGCTCTAGGCACCA-3′). Each PCR was done in duplicate and the experiment was repeated at least thrice (DNA Engine Opticon; MJ Research). Data were analyzed by Opticon-3 software and normalized to actin β (*ACTB*). Errors were calculated as previously described (44).

Cell Proliferation and Invasion

Cell proliferation was quantified using [^{3}H]thymidine incorporation as described in Supplementary Methods. Cells were analyzed for invasion through Matrigel chambers as described previously (46) and slightly modified (Supplementary Methods).

Cell Migration

Cell migration was measured by a wound assay as described previously (47). Briefly, the cells were seeded in 35 mm Petri dishes and cultured until confluence. The cells were then scraped with a 200 μL micropipette tip, denuding a strip of the monolayer. The cells were time-lapse–monitored every minute for 24 h in the set-up previously described (27). The uncovered wound area was measured and quantified at different intervals for 24 h with ImageJ 1.37v (NIH). The migration rate was calculated as the slope of free wound area/time.

RT-qPCR Microarrays

RNA from PC3, PC3HO-1, PC3pcDNA3, and MDA PCa2b were isolated as described above. Samples were then submitted to SuperArray Bioscience Corporation to perform RT-qPCR Oligo GEArray Human Angiogenesis Microarray analysis. One hundred and thirteen genes were analyzed. Data were normalized to B2M, HPRT1, RPL13A, GAPDH, and ACTB genes and two independent experiments were done. Genes with expression levels higher than 2 were considered upregulated and lower than −2 were considered repressed.

Human Prostate Cancer Xenograft Model

Six- to 8-wk-old male athymic nude (*nu/nu*) mice, each weighing at least 20 g, were purchased from CONEA (Comisión Nacional de Energía Atómica/Centro Atomico Ezeiza/U. A. Aplicaciones Tecnologicas Y Agropecuarias/Bioterio, Buenos Aires, Argentina). Mice were used in accordance with the "Guidelines for the Welfare of Animals in Experimental Neoplasia" (U.K. Coordinating Committee on Cancer Research). Mice were randomized into two groups: PC3HO-1 and PC3pcDNA3. Tumor cells (3.6 × 10^6 in 200 μL of RPMI) were injected s.c. in the right flank of athymic nude (*nu/nu*) male mice using a monoject 200 30-gauge × 1/2. Tumors were measured with a caliper starting at 8 d after inoculation, when the tumors became detectable under the skin. Their volumes were calculated using the formula $\pi/6 \times a \times b^2$, where *a* is the longest dimension of the tumor, and *b* is the width. Twenty-three days after xenograft generation, before euthanasia, mice were anesthetized and tumors excised. Harvested tumors were snap-frozen in liquid nitrogen and subsequently processed for immunohistochemistry and RNA isolation.

Immunohistochemical Analysis

All tumors were processed and fixed using routinely established protocols and stained as previously described (25). Briefly, immunohistochemistry was done using the streptavidin-biotin-peroxidase complex system LSAB + kit, horseradish peroxidase (DAKO). Endogenous peroxide activity was quenched

using hydrogen peroxide in distilled water (3%). Antigen retrieval was done by microwaving. Tissue slides were incubated overnight with the following primary antibodies: monoclonal mouse anti-MMP9 (1:400) from Santa Cruz Biotechnology and rabbit polyclonal anti–HO-1 (1:50) from Stressgen Biotechnologies Corp.; this was followed by sequential incubations with biotinylated link antibody and peroxidase-labeled streptavidin complex. The peroxidase reaction was conducted, under microscope, using 3,3′-diaminobenzidine. Slides were counterstained with Mayer's hematoxylin and analyzed by standard light microscopy. Negative control slides were prepared by substituting primary antiserum with PBS. For semiquantitative analysis, the degree of staining was rated as high, moderate, low, or not detectable (3+, 2+, 1+, and 0, respectively); the staining was also observed for localization. Five tumors in the PC3HO-1 group and five tumors in the PC3pcDNA3 group were analyzed.

Statistical Analysis

All results are given as mean ± SD of "n" separate independent experiments unless stated otherwise. Student's t tests were used to ascertain statistical significance with a threshold of $P < 0.05$. Comparisons for *in vivo* experiments were made with one-way ANOVA followed by Dunnett's test, with $P < 0.05$ as the criterion for statistical significance.

Disclosure of Potential Conflicts of Interest

We declare no conflict of interest.

References

1. Jemal A, Murray T, Ward E, et al. Cancer statistics, 2005. CA Cancer J Clin 2005;55:10–30.

2. De Marzo AM, Platz EA, Sutcliffe S, et al. Inflammation in prostate carcinogenesis. Nat Rev Cancer 2007;7:256–69.

3. Croci DO, Zacarias Fluck MF, Rico MJ, Matar P, Rabinovich GA, Scharovsky OG. Dynamic cross-talk between tumor and immune cells in orchestrating the immunosuppressive network at the tumor microenvironment. Cancer Immunol Immunother 2007;56:1687–700.

4. Darash-Yahana M, Pikarsky E, Abramovitch R, et al. Role of high expression levels of CXCR4 in tumor growth, vascularization, and metastasis. FASEB J 2004;18:1240–2.

5. Vicari AP, Caux C. Chemokines in cancer. Cytokine Growth Factor Rev 2002; 13:143–54.

6. Dong Z, Bonfil RD, Chinni S, et al. Matrix metalloproteinase activity and osteoclasts in experimental prostate cancer bone metastasis tissue. Am J Pathol 2005;166:1173–86.

7. Pratap J, Javed A, Languino LR, et al. The Runx2 osteogenic transcription factor regulates matrix metalloproteinase 9 in bone metastatic cancer cells and controls cell invasion. Mol Cell Biol 2005;25:8581–91.

8. Ames BN, Gold LS, Willett WC. The causes and prevention of cancer. Proc Natl Acad Sci U S A 1995;92:5258–65.

9. Otterbein LE, Soares MP, Yamashita K, Bach FH. Heme oxygenase-1: unleashing the protective properties of heme. Trends Immunol 2003;24: 449–55.

10. Berberat PO, Dambrauskas Z, Gulbinas A, et al. Inhibition of heme oxygenase-1 increases responsiveness of pancreatic cancer cells to anticancer treatment. Clin Cancer Res 2005;11:3790–8.

11. Lin HY, Juan SH, Shen SC, Hsu FL, Chen YC. Inhibition of lipopolysaccharide-induced nitric oxide production by flavonoids in RAW264.7 macrophages involves heme oxygenase-1. Biochem Pharmacol 2003;66:1821–32.

12. Vicente AM, Guillen MI, Habib A, Alcaraz MJ. Beneficial effects of heme oxygenase-1 up-regulation in the development of experimental inflammation induced by zymosan. J Pharmacol Exp Ther 2003;307:1030–7.

13. Datta PK, Koukouritaki SB, Hopp KA, Lianos EA. Heme oxygenase-1 induction attenuates inducible nitric oxide synthase expression and proteinuria in glomerulonephritis. J Am Soc Nephrol 1999;10:2540–50.

14. Willis D, Moore AR, Frederick R, Willoughby DA. Heme oxygenase: a novel target for the modulation of the inflammatory response. Nat Med 1996;2: 87–90.

15. Bussolati B, Ahmed A, Pemberton H, et al. Bifunctional role for VEGF-induced heme oxygenase-1 *in vivo*: induction of angiogenesis and inhibition of leukocytic infiltration. Blood 2004;103:761–6.

16. Prawan A, Kundu JK, Surh YJ. Molecular basis of heme oxygenase-1 induction: implications for chemoprevention and chemoprotection. Antioxid Redox Signal 2005;7:1688–703.

17. Nishie A, Ono M, Shono T, et al. Macrophage infiltration and heme oxygenase-1 expression correlate with angiogenesis in human gliomas. Clin Cancer Res 1999;5:1107–13.

18. Liu LG, Yan H, Zhang W, et al. Induction of heme oxygenase-1 in human hepatocytes to protect them from ethanol-induced cytotoxicity. Biomed Environ Sci 2004;17:315–26.

19. Busserolles J, Megias J, Terencio MC, Alcaraz MJ. Heme oxygenase-1 inhibits apoptosis in Caco-2 cells via activation of Akt pathway. Int J Biochem Cell Biol 2006;38:1510–7.

20. Tsuji MH, Yanagawa T, Iwasa S, et al. Heme oxygenase-1 expression in oral squamous cell carcinoma as involved in lymph node metastasis. Cancer Lett 1999;138:53–9.

21. Fang J, Sawa T, Akaike T, et al. *In vivo* antitumor activity of pegylated zinc protoporphyrin: targeted inhibition of heme oxygenase in solid tumor. Cancer Res 2003;63:3567–74.

22. Tsuchihashi S, Tamaki T, Tanaka M, et al. Pyrrolidine dithiocarbamate provides protection against hypothermic preservation and transplantation injury in the rat liver: the role of heme oxygenase-1. Surgery 2003;133: 556–67.

23. Mayerhofer M, Florian S, Krauth MT, et al. Identification of heme oxygenase-1 as a novel BCR/ABL-dependent survival factor in chronic myeloid leukemia. Cancer Res 2004;64:3148–54.

24. Hill M, Pereira V, Chauveau C, et al. Heme oxygenase-1 inhibits rat and human breast cancer cell proliferation: mutual cross inhibition with indoleamine 2,3-dioxygenase. FASEB J 2005;19:1957–68.

25. Sacca P, Meiss R, Casas G, et al. Nuclear translocation of haeme oxygenase-1 is associated with prostate cancer. Br J Cancer 2007;97:1683–9.

26. Venkateswaran V, Fleshner NE, Klotz LH. Modulation of cell proliferation and cell cycle regulators by vitamin E in human prostate carcinoma cell lines. J Urol 2002;168:1578–82.

27. Salierno M, Cabrera R, Filevich O, Etchenique R. Encapsulated Petri dish system for single-cell drug delivery and long-term time lapse microscopy. Anal Biochem 2007;371:208–14.

28. John A, Tuszynski G. The role of matrix metalloproteinases in tumor angiogenesis and tumor metastasis. Pathol Oncol Res 2001;7:14–23.

29. Poss KD, Tonegawa S. Reduced stress defense in heme oxygenase 1-deficient cells. Proc Natl Acad Sci U S A 1997;94:10925–30.

30. Kawashima A, Oda Y, Yachie A, Koizumi S, Nakanishi I. Heme oxygenase-1 deficiency: the first autopsy case. Hum Pathol 2002;33:125–30.

31. Yachie A, Toma T, Mizuno K, et al. Heme oxygenase-1 production by peripheral blood monocytes during acute inflammatory illnesses of children. Exp Biol Med (Maywood) 2003;228:550–6.

32. Jozkowicz A, Was H, Dulak J. Heme oxygenase-1 in tumors: is it a false friend? Antioxid Redox Signal 2007;9:2099–117.

33. Maines MD, Abrahamsson PA. Expression of heme oxygenase-1 (HSP32) in human prostate: normal, hyperplastic, and tumor tissue distribution. Urology 1996;47:727–33.

34. Was H, Cichon T, Smolarczyk R, et al. Overexpression of heme oxygenase-1 in murine melanoma: increased proliferation and viability of tumor cells, decreased survival of mice. Am J Pathol 2006;169:2181–98.

35. Kapturczak MH, Wasserfall C, Brusko T, et al. Heme oxygenase-1 modulates early inflammatory responses: evidence from the heme oxygenase-1-deficient mouse. Am J Pathol 2004;165:1045–53.

36. Zhang X, Shan P, Jiang D, et al. Small interfering RNA targeting heme oxygenase-1 enhances ischemia-reperfusion-induced lung apoptosis. J Biol Chem 2004;279:10677–84.

37. Lin Q, Weis S, Yang G, et al. Heme oxygenase-1 protein localizes to the nucleus and activates transcription factors important in oxidative stress. J Biol Chem 2007;282:20621–33.

38. Ortega N, Behonick DJ, Werb Z. Matrix remodeling during endochondral ossification. Trends Cell Biol 2004;14:86–93.

39. Aalinkeel R, Nair MP, Sufrin G, et al. Gene expression of angiogenic factors correlates with metastatic potential of prostate cancer cells. Cancer Res 2004;64: 5311–21.

40. Bin Hafeez B, Adhami VM, Asim M, et al. Targeted knockdown of Notch1 inhibits invasion of human prostate cancer cells concomitant with inhibition of matrix metalloproteinase-9 and urokinase plasminogen activator. Clin Cancer Res 2009;15:452–9.

41. Lin CW, Shen SC, Hou WC, Yang LY, Chen YC. Heme oxygenase-1 inhibits breast cancer invasion via suppressing the expression of matrix metalloproteinase-9. Mol Cancer Ther 2008;7:1195–206.

42. Elbashir SM, Lendeckel W, Tuschl T. RNA interference is mediated by 21- and 22-nucleotide RNAs. Genes Dev 2001;15:188–200.

43. Elbashir SM, Harborth J, Weber K, Tuschl T. Analysis of gene function in somatic mammalian cells using small interfering RNAs. Methods 2002;26: 199–213.

44. Quesada AR, Barbacid MM, Mira E, Fernandez-Resa P, Marquez G, Aracil M. Evaluation of fluorometric and zymographic methods as activity assays for stromelysins and gelatinases. Clin Exp Metastasis 1997;15: 26–32.

45. Smith JL, Freebern WJ, Collins I, et al. Kinetic profiles of p300 occupancy *in vivo* predict common features of promoter structure and coactivator recruitment. Proc Natl Acad Sci U S A 2004;101:11554–9.

46. Lang H, Lindner V, Saussine C, Havel D, Faure F, Jacqmin D. Microscopic venous invasion: a prognostic factor in renal cell carcinoma. Eur Urol 2000;38: 600–5.

47. Petit V, Boyer B, Lentz D, Turner CE, Thiery JP, Valles AM. Phosphorylation of tyrosine residues 31 and 118 on paxillin regulates cell migration through an association with CRK in NBT-II cells. J Cell Biol 2000;148: 957–70.